The Pyrenees: glacial landforms from the Bølling–Allerød Interstadial (14.6–12.9 ka)

Magali Delmas, Marc Oliva, Yanni Gunnell, Marcelo Fernandes, Théo Reixach, José Fernández-Fernández, Marc Calvet

PART IV. European glacial landforms from the Bølling–Allerød Interstadial (14.6–12.9 ka)

SECTION 2 European regions that were not covered by the EISC

Abstract: The Bølling–Allerød (B-A) Interstadial (14.6–12.9 ka) was a period of intense glacier recession in the Pyrenees. All available proxies indicate that environmental conditions became substantially wetter and warmer than during the preceding post-LGM interval between 18.9 and 14.6 ka (early Last Glacial to Interglacial transition, LGIT). Most of the Pyrenean trunk glaciers vanished, being confined to the cirques and promoting the onset of paraglacial rock slope failures and the formation of rock glaciers. At lower elevations, forest expansion promoted a sharp decrease in catchment erosion rates. Braided glaciofluvial stream channels narrowed and gave way to meandering river styles. The detailed chronology of deglaciation during those 1700 years of rapid change has been documented for only a very small number of valleys, mostly relying on ^{10}Be or ^{36}Cl exposure ages obtained from glacially-polished bedrock steps on valley floors, with also a few results from ice-marginal boulders and/or rock glaciers. A period of glacier re-expansion occurred at the end of the B-A Interstadial in response to decreasing temperatures heralding the Younger Dryas.

Key words: Bølling–Allerød Interstadial, moraine, terrestrial cosmogenic nuclide exposure dating, Pyrenees

38. The Pyrenees: glacial landforms from the Bølling–Allerød Interstadial (14.6–12.9 ka)

(Magali Delmas, Marc Oliva, Yanni Gunnell, Marcelo Fernandes, Théo Reixach, José M. Fernández-Fernández and Marc Calvet)

38.1. Evidence of intense and rapid warming

As elsewhere around the North Atlantic (Liu et al., 2009; Thiagarajan et al., 2014, Naughton et al., 2021) and throughout most of Europe (Palacios, 2021), the onset of the Bølling–Allerød Interstadial (hereafter B-A, i.e., GI-1 after Rasmussen et al., 2014) in the Pyrenees featured a peak of warmth, with temperatures similar to present-day values, followed by gradual cooling (Bernal-Wormull et al., 2021). These conditions favoured the retreat and collapse of some Northern Hemisphere ice sheets, particularly the Eurasian Ice Sheet (Brendryen et al., 2020), and drove accelerated deglaciation along the entire strike of the Pyrenean mountain range (Fernandes et al., 2021). All available proxies indicate that palaeoenvironmental conditions came very close to resembling those later prevalent during the Holocene.

On the western side of the range (Ostolo cave, 248 m a.s.l., Basque mountains), $\delta^{18}O$ values from stalagmites record a temperature change of roughly 7.5 °C in less than 50 years around 14.938 ± 0.040 ka (model age based on 61 U–Th data points; Bernal-Wormull et al., 2021). This sharp change was almost synchronous with the onset of GI-1 in Greenland ice cores (14.692 ± 0.186 ka; Rasmussen et al., 2014). In the central Pyrenees, summer palaeotemperatures during the last glacial-to-interglacial transition (LGIT: 18.9–11.7 ka) have been inferred from chironomids in the lacustrine sediment sequence at Ech, a palaeolake (710 m). Results suggest summer temperatures of 16–17.5 °C during the B-A (GI-1), a rise of 3 to 7 °C compared to the early LGIT (i.e., Oldest Dryas: 18.9–14.6 ka), with three short (~100 years) cooling spikes during the B-A (Millet et al., 2012). Warming of this magnitude is also recorded in marine core MD99–2646 (Gulf of Lion), where April–May SSTs rose from 12 to 19 °C around 15 cal ka BP (Melki et al., 2009).

Pollen records also confirm a significant rise in temperature and precipitation in the Pyrenees at the beginning of the B-A, with an expansion of *Betula* and *Juniperus* and a decline of *Chenopodiaceae* from 15–14.5 cal ka BP (synthesis in Jalut et al., 1992; Fletcher et al., 2010; Moreno et al., 2012, 2014). Steppe taxa nonetheless remained abundant (*Artemisia*, *Apiaceae*, *Poaceae*, *Rumex*), particularly under Mediterranean influence where xerophytic plants were most conspicuous. In the wake of *Betula*, the ingress of *Pinus* was progressively followed by *Quercus*, with *Juniperus* yielding to the advance of forest vegetation up to altitudes of ~1700 m on slopes of the northern massifs (Reille and Andrieu, 1993). As a result of these land-cover changes, catchment erosion rates decreased. On valley floors, stream channels narrowed and braided patterns gave way to single-channel meandering river styles (Stange et al., 2013, 2014; Delmas et al., 2015, 2018; Nivière et al., 2016; Mouchené et al., 2017; synthesis in Delmas, 2019).

Although the precise footprint of glaciation during the B-A in the Pyrenees has only been established for a few valleys, all existing evidence points to glacier recession already under way at the beginning of the B-A (Fig. 38.1 and Table 38.1), fully in step with climate warming trends recorded regionally and globally at that time. Evidence is mostly based on ^{10}Be and ^{36}Cl exposure ages obtained from glacially-polished bedrock steps on valley floors, with also a few exposure ages from moraines and rock glaciers (Pallàs et al., 2006, 2010; Delmas et al., 2008, 2011; Palacios et al., 2015a, 2015b, 2017; Andrés et al., 2018; Oliva et al., 2021; Reixach et al., 2021; Fernandes et al., 2021).

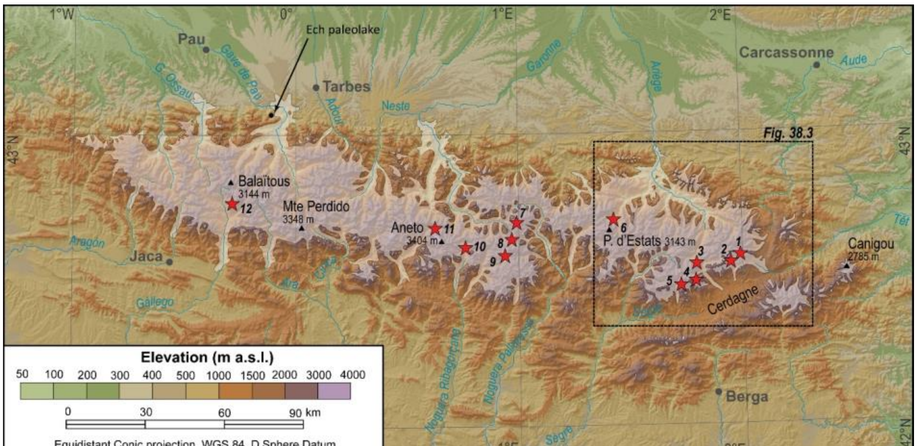

Figure 38.1. Spatial distribution of published research on the Bølling–Allerød Interstadial (14.6–12.9 ka) in the Pyrenees. *1- Grave/upper Têt valley (Delmas et al., 2008; Reixach et al., 2021). 2- SE Carlit/upper Têt valley (Delmas et al., 2008). 3- Orri/upper Querol valley (Pallàs et al., 2010; Reixach et al., 2021). 4- Malniu (Pallàs et al., 2010; Andrés et al., 2018; Reixach et al., 2021). 5- Arànser valley (Palacios et al., 2015a; Andrés et al., 2018; Reixach et al., 2021). 6- Médecourbe/upper Vicdessos valley; Jomelli et al., 2020; Reixach et al., 2021). 7- Bacivèr/Val d'Aran, i.e., upper Garonne valley (Oliva et al., 2021). 8- Ruda/Val d'Aran, i.e., upper Garonne valley (Fernandes et al., 2021). 9-*

Noguera de Tor (Copons and Bordonau, 1996). 10- Noguera Ribagorçana (Pallàs et al., 2006). 11- Ésera (Crest et al., 2017). 12- Gállego (Palacios et al., 2015b, 2017).

38.2. Almost full glacier extinction in the eastern Pyrenees

In the eastern massifs of the Pyrenees such as the southern flanks of the Tossa Plana and Campcardós, and likewise the SE Carlit, exposure ages from ice-marginal deposits have shown that the landscape had been entirely deglaciated at the beginning of the B-A, thereby promoting the onset of paraglacial rock slope failures and a proliferation of rock glaciers and, more locally, small debris-covered glaciers (Fig. 38.2).

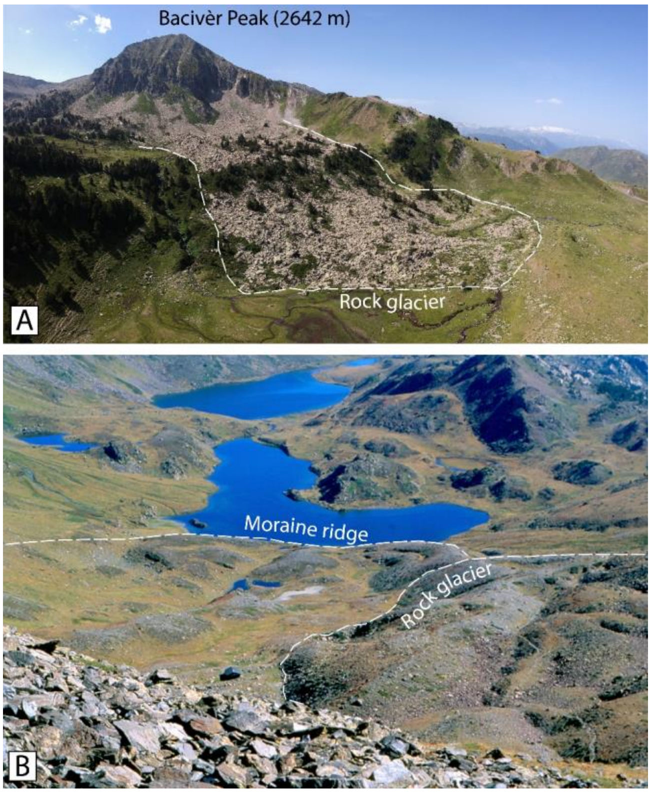

Figure 38.2. Rock glacier development at the time of the Bølling–Allerød Interstadial (14.6–12.9 ka).

A. Transitional landforms, including a debris-covered glacier (lower part) and a rock glacier (upper part), in the north-facing cirque of Bacivèr Peak (Noguera Pallaresa watershed). B. Moraine and rock glacier in an east-facing cirque of Pic Carlit (Têt watershed).

a mis en forme : Police :Gras, Italique

In the Campcardós massif, the last presence of cirque glaciers dates back to the early LGIT (GS-2.1a; see Chapter 21). Glacier extinction occurred there during the B-A (Pallàs et al., 2010, Andrés et al., 2018; Reixach et al. 2021). Given the elevation of those south-facing cirque floors (2420 to 2550 m), it can be inferred that the ELA was locally at least 2500 m. Among south-facing cirques of the neighbouring Carlit massif, exposure ages of 16.1 ± 2.0 ka, 16.9 ± 1.9 ka and 16.6 ± 2.4 ka were obtained from glacially-polished bedrock steps situated at 2350 and 2410 m (sites J and K, respectively, see Fig. 38.3 for exposure ages without snow correction). In the south-facing upper

Arànser valley (Tossa Plana massif), exposure ages of 13.7 ± 1.1 ka (PIR 11-12), 14.7 ± 1.4 ka (PIR 11-08), and 12.6 ± 1.1 ka (PIR 11-09) were obtained from rock glacier boulders situated at elevations ranging between 2150 and 2450 m (Palacios et al., 2015a; Andrés et al., 2018; Reixach et al., 2021).

The only evidence of surviving cirque glaciers is restricted to suitably snow-fed areas at high elevations. This also includes some S- or SE-facing cirques exposed to moist airflow from the northwest locally spilling over ridgetops. An example is the Grave (upper Têt valley), where a cirque glacier appears to have subsisted during the B-A (weighted mean ^{10}Be exposure ages of 13.8 ± 0.6 ka and 13.1 ± 0.6 ka obtained from two frontal moraines situated at elevations of 2150 and 2160 m; samples at sites M, N and O, Fig. 38.3; Delmas et al., 2008); and where the inferred ELA was ~2450 m (Reixach et al., 2021). Such was also the case in the upper Querol valley (Col de Puymorens), where NE-facing Orri Cirque hosted a valley glacier 3.8 km long, descending to an elevation of 2100 m, and with a local ELA around 2420 m (weighted mean age of 14.5 ± 0.6 ka based on exposure ages obtained from the corresponding lateral moraine: 14.4 ± 1.4 ka (LOR01), 15.0 ± 1.5 ka (LOR03), 13.7 ± 1.0 ka (LOR04), and 15.4 ± 1.9 ka (LOR05); Fig. 38.3; Pallàs et al., 2010; Reixach et al., 2021). Lastly, Médecourbe cirque (upper Soulcem valley, Ariège) hosted a 1.5 km long glacier with an ELA around 2525 m (weighted mean age of 13.2 ± 0.9 ka). Those results are based on four ^{10}Be exposure ages from a frontal moraine located at 2230 m (Fig. 38.3; Jomelli et al., 2020; Reixach et al., 2021).

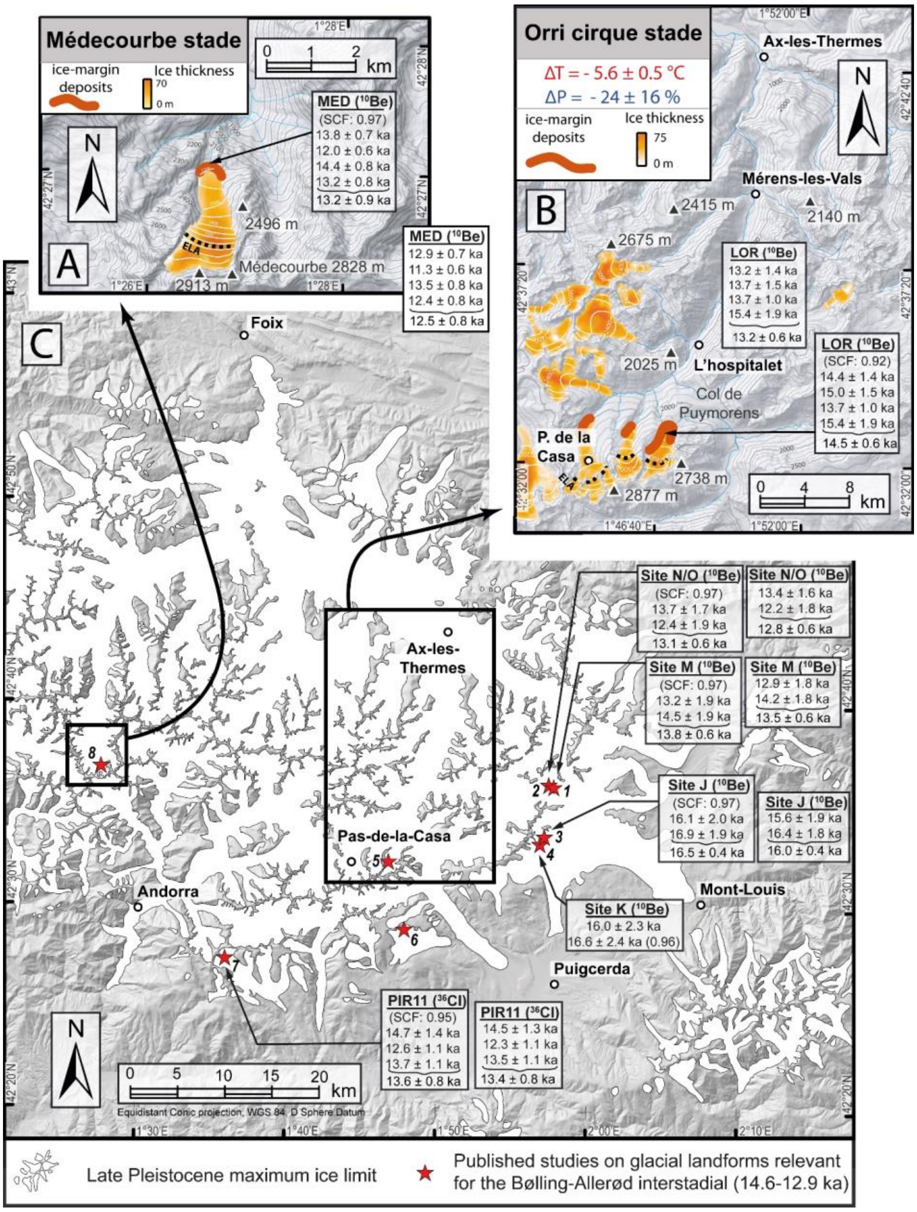

Figure 38.3. East Pyrenean ice extent at the time of the Bølling–Allerød Interstadial (14.6–12.9 ka). ***A.*** *Ice extent in Médecourbe cirque at the time of the Bølling–Allerød interstadial or Younger Dryas, depending of whether or not a snow correction factor is applied.* ***B.*** *Ice extent in Médecourbe cirque at the time of the Bølling–Allerød Interstadial and/or Younger Dryas.* ***C.*** *Location map. Red stars locate ^{10}Be and ^{36}Cl sampling sites: 1- Grave (upper Têt watershed), frontal moraine at 2150 m, site M (Delmas et al., 2008; ages recalculated after Reixach et al., 2021). 2- Grave (upper Têt valley), frontal*

moraine at 2160 m, sites N and O (Delmas et al., 2008; ages remodelled after Reixach et al., 2021). 3- SE Carlit (upper Têt watershed), bedrock step at 2350 m (site J; Delmas et al., 2008; ages remodelled for this review). 4- SE Carlit (upper Têt watershed), bedrock step at 2410 m, site K (Delmas et al., 2008), ages remodelled for this review). 5- Orri (upper Querol watershed), lateral moraine, site LOR (Pallàs et al., 2010; ages remodelled after Reixach et al., 2021). 6- Malniu (Pallàs et al., 2010; Andrés et al., 2018; ages remodelled after Reixach et al., 2021). 7- Arànser, rock glacier, site PIR11 (Palacios et al., 2015a; Andrés et al., 2018; ages remodelled after Reixach et al., 2021). 8-Médecourbe (upper Vicdessos valley), frontal moraines, site 'Med' (Jomelli et al., 2020; ages remodelled after Reixach et al., 2021). Exposure ages with and without a snow correction factor (SCF values indicated in brackets) are presented in separate boxes, with weighted mean ages displayed below the curly bracket. For site K, exposure ages are reported without (top) and with (bottom) a snow correction factor (SCF value indicated in brackets).

38.3. Extensive glacier recession in the western and central Pyrenees

^{10}Be exposure ages from two glacial cirques in the headwaters of the upper Garonne valley (Val d'Aran) confirm the regional indices of rapid warming presented in Section 38.1. Samples obtained from polished bedrock surfaces from the lip (1950–2000 m), floor (2200–2300 m) and upper headwalls (2400–2440 m) of Bacivèr Cirque, for example, document rapid retreat between 14.8 and 14.2 ka (Oliva et al., 2021). The data also suggest full deglaciation of this west-facing cirque (local peaks around 2600–2650 m) by the end of the B-A, with local variants further addressed in Section 38.4. A similar process occurred in tributary watersheds of the Ebro River, such as in small cirques of the upper Gállego valley where valleys sub-catchments at elevations of ~2600–2700 m were apparently also glacier-free by 14 ka (Palacios et al., 2015b). Deglaciation promoted very active paraglacial dynamics inside the recently ice-free cirques, leading to the formation of permafrost-related landforms such as rock glaciers on cirque slopes (Palacios et al., 2017).

The last remaining valley glaciers likewise vanished from the Ésera and Noguera Ribagorçana valleys by the end of the B-A, confining residual glaciers thereafter to the cirques (Pallàs et al., 2006; Crest et al., 2017). A widespread population of lakes also became a feature in the most elevated cirques. Sediment cores from Lake Redó (Noguera de Tor valley), for example, have yielded a record of glacio-lacustrine sedimentation beginning around 13,470 ± 60 yr BP (16,068 to 16,481 cal yr BP) and continuing until the early Holocene, as shown by a radiocarbon age of 9,880 ± 60 yr BP (11,243 to 11,457 cal yr BP) obtained from gyttja deposits in the stratigraphy (Copons and Bordonau, 1996).

38.4. Local evidence of glacial oscillations in the higher central part of the mountain range

Greenland ice cores recorded several cold phases during the LGIT, such as the Older Dryas or the Intra-Allerød Cold Period, nested within the warmer B-A interval (Rasmussen et al., 2014). The regional trend of glacier recession in the Pyrenees likewise recorded short periods of centennial-scale cooling at Ech palaeolake (710 m; Millet et al., 2012), Lake Estanya (670 m; Vegas-Vilarrúbia et al., 2013), and in the Portalet sedimentary fill sequence (1802 m, uppermost Gállego watershed; González-Sampériz et al., 2006). These colder spikes may have promoted glacier expansion among north-facing cirques of the central Pyrenees in areas surrounded by high peaks (> 2800 m) and benefiting from suitably large accumulation zones above 2400–2500 m. This would have favoured the persistence, and perhaps the readvance, of short cirque glaciers (< 1 km) in the lower elevation belts of the central and western Pyrenees, with glaciers expanding to greater lengths (< 3–5 km) in the vicinity of higher peaks. In Piniecho Cirque (upper Gállego valley), for example, moraines from the late B-A have been found extending 0.4–0.6 km from the headwall at elevations of 2300–2350 m (elevation of surrounding ridgetops: ~2700 m; Palacios et al., 2017).

As in the eastern Pyrenees (Section 38.2), local topoclimatic conditions must have played a prominent role in the magnitude, distribution, and chronology of glacier behaviour during the B-A, but with additional evidence of glacier response to the colder oscillations. Ages of 14.8 and 14.0 ka, for example, were obtained from polished surfaces at lower altitudes (1860–1900 m) on the floor of Ruda valley (uppermost Garonne watershed; Fernandes et al., 2021), where glacier retreat and ice thinning during the B-A were interrupted by two brief stillstands (perhaps even involving a minor readvance), with corresponding moraine ages of 13.5 and 13.0 ka (Fernandes et al., 2021). Bacivèr cirque recorded a similar trend, with moraines 0.3 km from the headwall corresponding to a stillstand around 12.9 ka (Oliva et al., 2021), and thus also heralding the onset of the Younger Dryas.

38.5. Conclusion

Despite the limited chronological constraints on the glacial landforms generated during the B-A Interstadial, it appears that glacier behaviour between 14.6 and 12.9 ka was relatively uniform along and across the Pyrenean range. The period recorded a major glacier recession phase as early as 15–14 ka (transition between GS-2.1a and GI-1) caused by a rise of ELAs by about 100 m with respect to their earlier LGIT positions (Table 38.1). This trend matches the Greenland ice stratigraphic record as well as all climatic and environmental proxies recorded regionally. Brief glacier stillstands and/or advances recorded at a small number of locations in the higher central ranges also occurred in step with colder oscillations of the B-A interval such as the Older Dryas and the Intra-Allerød Cold Period.

Table 38.1. Glaciated environments in the Pyrenees during the Bølling–Allerød Interstadial (14.6–12.9 ka): a summary

Valley (massif or cirque)	Climatic conditions	Age of maximum glacier extent (ka)	Proportion of ice cover (at maximum extent) relative to LGM (%)	ELA at time of B-A (m)	Glacier-front elevation at maximum extent (m)	Main landforms	Key publications
Arànser (Tossa Plana)	Warm and humid (close to present-day conditions)	Cirque glaciers became extinct during the B-A. Period of rock glacier development (regional ELA > 2500 m)					Palacios et al., 2015a; Andrés et al., 2018; Reixach et al., 2021
Malniu (Campcardós)		Cirque glaciers became extinct during the B-A (regional ELA > 2500 m)					Pallàs et al., 2010; Andrés et al., 2018; Reixach et al., 2021
Grave (Carlit)		13.8 ± 0.6	5	2450	2150	Frontal moraine	Delmas et al., 2008; Reixach et al., 2021

Querol valley (Orri)		14.5 ± 0.6	3	2420	2100	Lateral and frontal moraines	Pallàs et al., 2010; Reixach et al., 2021
Soulcem/Ariège (Médecourbe)		13.2 ± 0.9	3	2525	2230	Frontal moraine	Jomelli et al., 2020; Reixach et al., 2021
Upper Gállego		Ice-free at ~2600–2700 m after 14 ka					Palacios et al., 2015b, 2017
Val d'Aran (Bacivèr)	Warm	15–14	5	-	1950	Polished surfaces	Oliva et al., 2021
Val d'Aran/upper Garonne (Ruda)	Warm	15–14	5	-	1860–1900	Polished surfaces	Fernandes et al., 2021
Val d'Aran/upper Garonne (Ruda)	Short cold spike	13.5	4	2460	2080	Frontal moraine	Fernandes et al., 2021

References

Andrés, N., Gómez-Ortiz, A., Fernández-Fernández, J.M., Tanarro, L.M., Salvador-Franch, F., Oliva, M., Palacios, D., 2018. Timing of deglaciation and rock glacier origin in the southeastern Pyrenees: a review and new data. Boreas 47, 1050–1071.

Bernal-Wormull, J.L., Moreno, A., Bartolomé, M., Aranburu, A., Arriolabengoa, M., Iriarte, E., Cacho, I., Spötl, C., Edwards, R.L., Cheng, H., 2021. Immediate temperature response in northern Iberia to last deglacial changes in the North Atlantic. Geology 49, 6–10.

Brendryen, J., Haflidason, H., Yokoyama, Y., Haaga, K.A., Hannisdal, B., 2020. Eurasian Ice Sheet collapse was a major source of Meltwater Pulse 1A 14,600 years ago. Nature Geoscience 13, 363–368.

Copons, R., Bordonau, J., 1996. El registro sedimentario del Cuaternario Reciente en el lago Redó d'Aigüestortes (Pirineos Centrales), in: Grandal, A., Pagés, J. (Eds.), IV Reunión de Geomorfología. Sociedad Española de Geomorfología.

Crest, Y., Delmas, M., Braucher, R., Gunnell, Y., Calvet, M., 2017. Cirques have growth spurts during deglacial and interglacial periods: Evidence from ^{10}Be and ^{26}Al nuclide inventories in the central and eastern Pyrenees. Geomorphology 278, 60–77.

Delmas, M., Gunnell, Y., Braucher, R., Calvet, M., Bourlès, D. 2008. Exposure age chronology of the last glacial cycle in the eastern Pyrenees. Quaternary Research 69, 231–241.

Delmas, M., Calvet, M., Gunnell, Y., Braucher, R., Bourlès, D., 2011. Palaeogeography and ^{10}Be exposure-age chronology of Middle and Late Pleistocene glacier systems in the northern Pyrenees: implications for reconstructing regional palaeoclimates. Palaeogeography, Palaeoclimatology, Palaeoecology 305, 109–122.

Delmas, M., Braucher, R., Gunnell, Y., Guillou, V., Calvet, M., Bourlès, D., 2015. Constraints on Pleistocene glaciofluvial terrace age and related soil chronosequence features from vertical ^{10}Be profiles in the Ariège River catchment (Pyrenees, France). Global and Planetary Change132, 39–53.

Delmas, M., Calvet, M., Gunnell, Y., Voinchet, P., Manel, C., Braucher, R., Tissoux, H., Bahain, J.J., Perrenoud, C., Saos, T., 2018. Terrestrial ^{10}Be and Electron Spin Resonance dating of fluvial terraces quantifies Quaternary surface uplift in the eastern Pyrenees. Quaternary Science

Reviews 193, 188–211.

Delmas, M., 2019. L'apport des nucléides cosmogéniques produits in situ à la quantification multi-scalaire des changements environnementaux quaternaires dans les montagnes des latitudes tempérées. Mémoire d'Habilitation à Diriger des Recherches, Université Lumière Lyon 2, 312 p.

Fernandes, M., Oliva, M., Vieira, G., Palacios, D., Fernández-Fernández, J.M., Garcia-Oteyza, J., Schimmelpfennig, I., Team, A., Antoniades, D., 2021. Glacial oscillations during the Bølling-Allerød Interstadial-Younger Dryas transition in the Ruda Valley, Central Pyrenees. Journal of Quaternary Science, 1–17, https://doi.org/10.1002/jqs.3379.

Fletcher, W.J., Sánchez Goñi, M.F., Allen, J.R.M., Cheddadi, R., Combourieu-Nebout, N., Huntley, B., Lawson, I., Londeix, L., Magri, D., Margari, V., Müller, U.C., Naughton, F., Novenko, E., Roucoux, K., Tzedakis, P.C., 2010. Millenial-scale variability during the last glacial in vegetation records. Quaternary Science Reviews 29, 2839–2864.

González-Sampériz, P., Valero-Garcés, B.L., Moreno, A., Jalut, G., García-Ruiz, J.M., Martí-Bono, C., Delgado-Huertas, A., Navas, A., Otto, T., Dedoubat, J.J., 2006. Climate variability in the Spanish Pyrenees during the last 30,000 yr revealed by the El Portalet sequence. Quaternary Research 66, 38–52.

Jalut, G., Montserrat Marti, J., Fontugne, M., Delibrias, G., Vilaplana, J.M., Julia, R., 1992. Glacial to Interglacial vegetation changes in the northern and southern Pyrenees: deglaciation, vegetation cover and chronology. Quaternary Science Reviews 11, 449–480.

Liu, Z., Otto-Bliesner, B.L., He, F., Brady, E.C., Tomas, R., Clark, P.U., Carlson, A.E., Lynch-Stieglitz, J., Curry, W., Brook, E., Erickson, D., Jacob, R., Kutzbach, J., Cheng, J., 2009. Transient simulation of last deglaciation with a new mechanism for Bølling–Allerød warming. Science 325, 310–314. https://doi.org/10.1126/science.1171041

Millet, L., Rius, D., Galop, D., Heiri, O., Brooks, S.J., 2012. Chironomid-based reconstruction of Lateglacial summer temperatures from the Ech palaeolake record (French western Pyrenees). Palaeogeography, Palaeoclimatology, Palaeoecology 315–316, 86–99. https://doi.org/10.1016/j.palaeo.2011.11.014

Moreno, A., González-Sampériz, P., Morellón, M., Valero-Garcés, B.L., Fletcher, W.J., 2012. Northern Iberian abrupt climate change dynamics during the last glacial cycle: a view from lacustrine sediments. Quaternary Science Reviews 36, 139–153.

Moreno, A., Svensson, A., Brooks, S.J., Connor, S., Engels, S., Fletcher, W., Genty, D., Heiri, O., Labuhn, I., Persoiu, A., Peyron, O., Sadori, L., Valero-Garces, B., Wulf, S., Zanchetta G., 2014. A compilation of Western European terrestrial records 60e8 ka BP: towards an understanding of latitudinal climatic gradients. Quaternary Science Reviews 106, 167–185.

Mouchene, M., van der Beek, P., Mouthereau, F., Carcaillet, J., 2017. Controls on quaternary incision of the northern pyrenean foreland: chronological and geomorphological constraints from the lannemezan megafan, SW France. Geomorphology 281, 78–93.

Naughton, F., Toucanne, S., Landais, A., Rodrigues, T., Vazquez Riveiros, N., Sánchez Goñi, M.F., 2021. The Bølling-Allerød Interstadial (chapter 6). In: Palacios, D., Hughes, P., García-Ruiz, J.M., Andrés, A. (Eds.), European Glacial Landscapes: Maximum Extent of Glaciations. Elsevier (in press).

Nivière, B., Lacan, P., Regard, V., Delmas, M., Calvet, M., Huyghe, D., Roddaz, B., 2016. Evolution of the late Pleistocene Aspe river (western Pyrenees, France). Signature of climatic events and active tectonics. Compte Rendus Geoscience 348, 203–212.

Oliva, M., Fernandes, M., Palacios, D., Fernández-Fernández, J.M.J.-M., Schimmelpfennig, I., Antoniades, D., Aumaître, G., Bourlès, D., Keddadouche, K., Team, A.S.T.E.R., Antoniades, D., 2021. Rapid deglaciation during the Bølling-Allerød Interstadial in the Central Pyrenees and associated glacial and periglacial landforms. Geomorphology 385, 107735. https://doi.org/10.1016/j.geomorph.2021.107735

Palacios, D., de Andrés, N., Gómez-Ortiz, A., García-Ruiz, J.M., 2017. Evidence of glacial activity during the Oldest Dryas in the mountains of Spain. Geological Society Special Publication 433, 87–110.

Palacios, D., Gómez-Ortiz, A., de Andrés, N., Vázquez-Selem, L., Salvador-Franch, F., Oliva, M. 2015a. Maximum Extent of Late Pleistocene Glaciers and Last Deglaciation of La Cerdanya Mountains, Southeastern Pyrenees. Geomorphology 231, 116–129.

Palacios, D., de Andrés, N., López-Moreno, J.I., García-Ruiz, J.M., 2015b. Late Pleistocene deglaciation in the upper Gállego Valley, central Pyrenees. Quaternary Research 83, 397–414.

Palacios, D., 2021. Concept and global context of the glacial landforms from the Bølling-Allerød Interstadial. In: Palacios, D., Hughes, P., García-Ruiz, J.M., Andrés, A. (Eds.), European Glacial Landscapes: Maximum Extent of Glaciations. Elsevier (in press).

Pallàs, R., Rodés, A., Braucher, R., Carcaillet, J., Ortuño, M., Bordonau, J., Bourlès, D., Vilaplana, J.M., Masana, E., Santanach, P., 2006. Late Pleistocene and Holocene glaciation in the Pyrenees: a critical review and new evidence from ^{10}Be exposure ages, south-central Pyrenees. Quaternary Science Reviews 25, 2937–1963.

Pallàs, R., Rodés, A., Braucher, R., Bourlès, D., Delmas, M., Calvet, M., Gunnell, Y., 2010. Small, isolated glacial catchments as priority targets for cosmogenic surface exposure dating of Pleistocene climate fluctuations, southeastern Pyrenees. Geology 38, 891–894.

Rasmussen, S.O., Bigler, M., Blockley, S.P., Blunier, T., Buchardt, S.L., Clausen, H.B., Cvijanovic, I., Dahl-Jensen, D., Johnsen, S.J., Fischer, H., Gkinis, V., Guillevic, M., Hoek, W.Z., Lowe, J.J., Pedro, J.B., Popp, T., Seierstad, I.K., Steffensen, J.P., Svensson, A.M., Vallelonga, P., Vinther, B.M., Walker, M.J.C., Wheatley, J.J., Winstrup, M., 2014. A stratigraphic framework for abrupt climatic changes during the Last Glacial period based on three synchronized Greenland ice-core records: Refining and extending the INTIMATE event stratigraphy. Quaternary Science Reviews 106, 14–28.

Reille, M., Andrieu, V., 1993. Variations de la limite supérieure des forêts dans les Pyrénées (France) pendant le Tardiglaciaire. Compte rendu de l'Académie des Sciences de Paris Série II 316, 547–551.

Reixach, T., Delmas, M., Braucher, R., Gunnell, Y., Mahé, C., Calvet, M. 2021. Climatic conditions between 19 and 12 ka in the eastern Pyrenees, and wider implications for atmospheric circulation patterns in Europe. Quaternary Science Reviews 260, https://doi.org/10.1016/j.quascirev.2021.106923

Stange, K.M., Van Balen, R.T., Carcaillet, J., Vandenberghe, J., 2013. Terrace staircase development in the southern Pyrenees foreland: inferences from ^{10}Be terrace exposure ages at the Segre River. Global Planet. Change 101, 97–112.

Stange, K.M., Van Balen, R.T., Kasse, C., Vandenberghe, J., Carcaillet, J., 2014. Linking morphology across the glaciofluvial interface: a ^{10}Be supported chronology of glacier advances and terrace formation in the Garonne River, northern Pyrenees, France. Geomorphology 207, 71–95.

Thiagarajan, N., Subhas, A. V., Southon, J.R., Eiler, J.M., Adkins, J.F., 2014. Abrupt pre-Bølling-Allerød warming and circulation changes in the deep ocean. Nature 511, 75–78.

Vegas-Vilarrúbia, T., González-Sampériz, P., Morellón, M., Gil-Romera, G., Pérez-Sanz, A., Valero-Garcés, B., 2013. Diatom and vegetation responses to Late Glacial and Early Holocene climate changes at Lake Estanya (Southern Pyrenees, NE Spain). Palaeogeography, Palaeoclimatology, Palaeoecology 392, 335–349.